Volume 27
Number 19
21 May 2025
Pages 2955–3154

CrystEngComm

rsc.li/crystengcomm

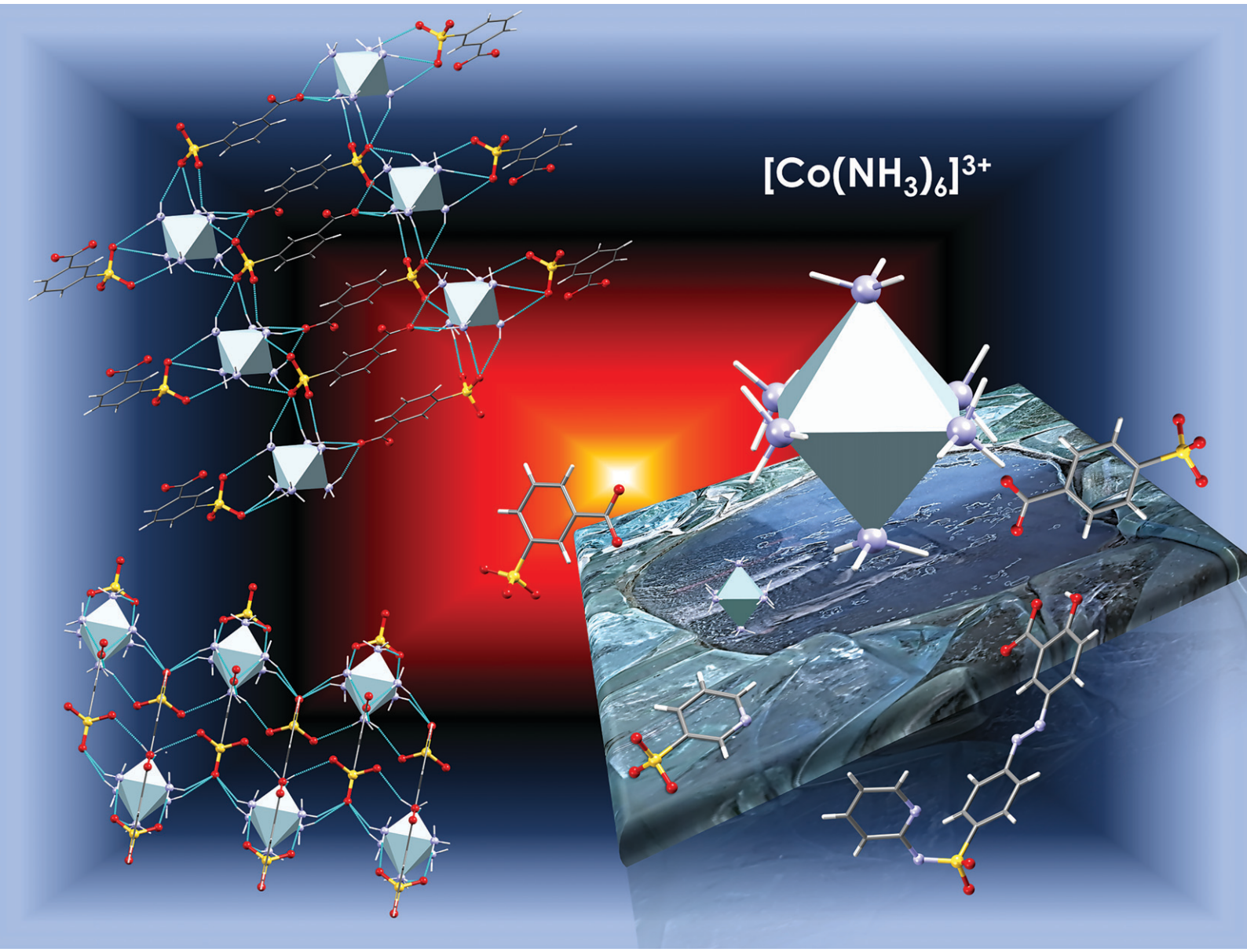

ISSN 1466-8033

ROYAL SOCIETY OF CHEMISTRY

PAPER

Svetlana G. Baca *et al.*

Multi-component supramolecular compounds containing hexaamminecobalt(III) cations and aromatic sulfonic acid derivatives

CrystEngComm

ROYAL SOCIETY OF CHEMISTRY

PAPER

View Article Online
View Journal | View Issue

Cite this: *CrystEngComm*, 2025, **27**, 3018

Multi-component supramolecular compounds containing hexaamminecobalt(III) cations and aromatic sulfonic acid derivatives†

Ecaterina S. Beleaev, Victor Ch. Kravtsov, Yurii Chumakov and Svetlana G. Baca *

A series of new multi-component supramolecular compounds containing $[Co(NH_3)_6]^{3+}$ cations and aromatic sulfonic acid derivatives has been synthesized and characterized using elemental analysis, FT-IR spectroscopy, and single-crystal X-ray diffraction. The series includes $[Co(NH_3)_6](pys)_3{\cdot}Hpys$ (**1**), $[Co(NH_3)_6](pys)_2Cl{\cdot}2MeCN$ (**2**), $[Co(NH_3)_6](3\text{-sb})Cl{\cdot}4H_2O$ (**3**), $[Co(NH_3)_6]_2(3\text{-sb})(SO_4)Cl_2{\cdot}7H_2O$ (**4**), $\{[Co(NH_3)_6][Na(3\text{-sb})Cl_2]{\cdot}H_2O\}_n$ (**5**), $\{[Co(NH_3)_6][K_2(4\text{-sb})_2Cl]\}_n$ (**6**), and $[Co(NH_3)_6](Hssz)(ssz){\cdot}4H_2O$ (**7**) (where Hpys = 3-pyridinesulfonic acid, H_2sb = 3-/4-sulfobenzoic acid, H_2ssz = sulfasalazine). Single-crystal X-ray diffraction analysis reveals that the compounds are ionic and multi-component, with complex $[Co(NH_3)_6]^{3+}$ cations forming hydrogen bonds with anions and solvate molecules. The presence of alkali metal cations in the crystals of **5** and **6** leads to the formation of anionic coordination polymers, 1D in **5** and 3D in **6**, which are H-bonded to complex $[Co(NH_3)_6]^{3+}$ cations. Hirshfeld surface analysis and 2D fingerprint plots demonstrate that the hexaamminecobalt(III) cation exhibits significant hydrogen bond capability when co-crystallized with derivatives of sulfonic acid, and in addition to hydrogen bonds of N–H···O type between the amine ligands and the sulfonate groups, π···π stacking and C–H···π interactions contribute significantly in stabilizing the supramolecular architectures. Energy decomposition analysis of the intermolecular interaction energy was performed using the SAPT method to study the non-covalent bonding interactions of $[Co(NH_3)_6]^{3+}$ cations with various aromatic sulfonic acid derivatives in **1**–**7**.

Received 19th February 2025,
Accepted 8th April 2025

DOI: 10.1039/d5ce00184f

rsc.li/crystengcomm

Introduction

Cobalt is an essential element for biological systems due to its key role in the formation of vitamin B12. In living organisms, it is involved in the formation or activation of enzymes, vitamins, and hormones and regulates metabolism. In this context, the synthesis and study of new cobalt compounds, which theoretically can be used to create and study systems that modulate biological functions, are relevant. Until now, the main efforts of the scientific community have been focused on the development of Co(II) complexes with biologically active ligands as excellent anticancer and antimicrobial agents.[1–3] Much less attention has been paid to Co(III) complexes, which also exhibit good antimicrobial activities and can be used as antiviral and antibacterial drugs.[2–9] For example, various Co(III)-based complexes have been tested against bacterial species such as *Staphylococcus aureus*, *Staphylococcus faecalis*, *Salmonella typhimurium*, *Bacillus subtilis*, *Proteus vulgaris*, *Pseudomonas*, *Pseudomonas aeruginosa*, and *Escherichia coli* and showed potent activity against standard and pathogenic resistant bacteria used.[10–13] In addition, Co(II/III) complexes offered advantages for medical imaging applications as MRI contrast agents and fluorescent probes.[1]

An important role in the manifestation of the properties of cobalt-based compounds is played by ligands, which can stabilize a particular oxidation state of the metal through a wide range of donor atoms as well as form additional non-covalent interactions in the solids. The formation of non-covalent interactions, particularly hydrogen bonding networks, allows fine-tuning of the chemical and physical properties of the resulting solid materials.[14] The hexaamminecobalt(III) cation, $[Co(NH_3)_6]^{3+}$, is a unique donor of multiple hydrogen bonds through its six coordinated NH_3

Institute of Applied Physics, Moldova State University, Academiei 5, MD-2028 Chisinau, R. Moldova. E-mail: sbaca_md@yahoo.com, svetlana.baca@ifa.usm.md

† Electronic supplementary information (ESI) available: Table S1. $[Co(NH_3)_6]$-based compounds; Table S2. Crystal data and details of structural determinations for **1**–**7**; Table S3. Selected bond distances (Å) and angles (deg) in **1**–**7**; Table S4. Details of the hydrogen bonding interactions in **1**–**7**; Table S5. SAPT decomposition of the interaction energies; Fig. S1. IR spectrum of $[Co(NH_3)_6]Cl_3$; Fig. S2–S8. IR spectra of **1**–**7**; Fig. S9–S15. Additional details in the structures of **1**–**7**; Fig. S16–S18. Hirshfeld surface; Fig. S19. 2D fingerprint plots; Fig. S20. View of all selected pairs for estimation of their interaction energies. CCDC 2415770–2415776. For ESI and crystallographic data in CIF or other electronic format see DOI: https://doi.org/10.1039/d5ce00184f

groups[15–39] and has the ability to form a stable supramolecular framework in numerous multi-component compounds with different organic moieties (Table S1†). Recently, we have shown that the bulky $[Co(NH_3)_6]^{3+}$ cations serve as a structure-organizing component involving all eighteen H-atoms without exception in hydrogen bonds with anions or with neutral and solvent molecules in a family of multi-component crystalline compounds.[40] Biological studies of these compounds against the oncogenic bacterium *Rhizobium* (*Agrobacterium*) *vitis* demonstrated the efficacy of the multi-component solids, and the compound comprising hexaamminecobalt(III) chloride and 1,10-phenanthroline showed the highest inhibitory potential and is therefore qualified for application against bacterial cancer in plants.

In continuation of our research on the development of multi-component solids with biological properties, we report here the synthesis of a new series of compounds comprising the $[Co(NH_3)_6]^{3+}$ cation and aromatic sulfonic acid derivatives. The sulfonic acid derivatives bearing SO_3^- groups have a great tendency to form hydrogen bonds, thereby facilitating the formation of a diverse array of supramolecular motifs,[41–43] which is confirmed by the results from previous studies of compounds incorporating $[Co(NH_3)_6]^{3+}$ cations and organic sulfonate anions.[18–20,25,27,30,31] The prepared series includes the following compounds: $[Co(NH_3)_6](pys)_3{\cdot}Hpys$ (**1**), $[Co(NH_3)_6](pys)_2Cl{\cdot}2MeCN$ (**2**), $[Co(NH_3)_6](3\text{-sb})Cl{\cdot}4H_2O$ (**3**), $[Co(NH_3)_6]_2(3\text{-sb})(SO_4)Cl_2{\cdot}7H_2O$ (**4**), $\{[Co(NH_3)_6][Na(3\text{-sb})Cl_2]{\cdot}H_2O\}_n$ (**5**), $\{[Co(NH_3)_6][K_2(4\text{-sb})_2Cl]\}_n$ (**6**), and $[Co(NH_3)_6](Hssz)(ssz){\cdot}4H_2O$ (**7**) (where Hpys = 3-pyridinesulfonic acid, H_2sb = 3-/4-sulfobenzoic acid, H_2ssz = sulfasalazine, Scheme 1). The structures of all compounds have been solved by single-crystal X-ray diffraction, and additional insight into the nature and strength of the interactions between the components of the compounds has been provided by Hirshfeld surface analysis. Energy decomposition analysis of the intermolecular interaction energy (E_{int}) has been performed for pairs of complex cations and anions, which are linked by hydrogen bonds.

Experimental

All manipulations were performed under aerobic conditions using chemicals and solvents as received without further purification. IR spectra were recorded on a PerkinElmer Spectrum Series 815 FT-IR spectrometer in the 650–4000 cm^{-1} region (Fig. S1–S8†). An Elmasonic P ultrasonic bath operating at 37 kHz was used for ultrasonic irradiation. In the case of solvothermal syntheses, the reaction mixtures were placed in a sealed PTEE-lined steel autoclave. The temperature program started with heating from room temperature up to 80 °C within 1 h, the temperature was held constant for 6 h and then slowly cooled to room temperature within 12 h.

Synthesis of $[Co(NH_3)_6](pys)_3{\cdot}Hpys$ (1)

To a solution of 0.01 g (0.037 mmol) $[Co(NH_3)_6]Cl_3$ and 0.011 g (0.07 mmol) 3-pyridinesulfonic acid in 8 mL water, 0.01 g (0.067 mmol) triethanolamine was added. The resulting solution was stirred for 30 min at a temperature of 50 °C and filtered. The yellow filtrate was kept in a closed vial to allow the solvent to evaporate slowly at room temperature. Orange, small, round crystals **1** suitable for X-ray analysis, formed after 6 months, were filtered, washed with water and air-dried. Yield: 0.006 g (43% based on 3-pyridinesulfonic acid). FT-IR (cm^{-1}): 3159 m, 1570 m, 1395 sh, 1354 m, 1326 s, 1190 m, 1149 sh, 1096 w, 1024 w, 1007 sh, 915 sh, 825 m, 755 sh, 699 sh.

Synthesis of $[Co(NH_3)_6](pys)_2Cl{\cdot}2MeCN$ (2)

To a solution of 0.01 g (0.037 mmol) $[Co(NH_3)_6]Cl_3$ and 0.011 g (0.07 mmol) 3-pyridinesulfonic acid in 8 mL MeOH/MeCN

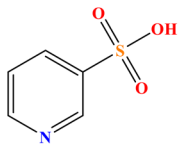

3-pyridinesulfonic acid

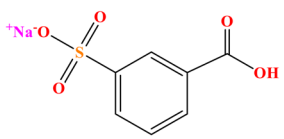

sodium salt of 3-sulfobenzoic acid

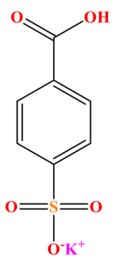

potassium salt of 4-sulfobenzoic acid

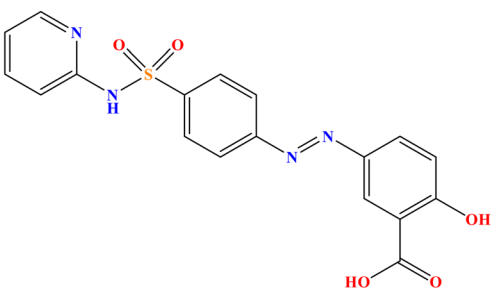

sulfasalazine

Scheme 1 Schematic representation of the aromatic sulfonic acid derivatives used in the synthesis of **1**–**7**.

(1 : 1) mixture, 0.01 g (0.067 mmol) triethanolamine was added. The resulting solution was ultrasonicated at 50 °C for 30 min and then filtered. The filtered mixture was placed in a vial and covered with a plastic cap to allow slow evaporation at room temperature. Orange needle-like crystals **2** suitable for X-ray analysis were filtered after 2 weeks, washed with acetonitrile and dried in air. Yield: 0.005 g (24% based on 3-pyridinesulfonic acid). Elemental analysis calcd for **2**, $C_{14}H_{32}ClCoN_{10}O_6S_2$ (594.99 g mol^{-1}): C, 28.26; H, 5.42; N, 23.54%. Found. C, 27.96; H, 5.14; N, 23.22%. IR (cm^{-1}): 3299 m, 1623 m, 1577 m, 1420 m, 1400 m, 1341 m, 1327 m, 1188 s, 1136 sh, 1043 m, 1007 s, 915 sh, 873 m, 857 m, 745 m.

Synthesis of $[Co(NH_3)_6](3\text{-sb})Cl{\cdot}4H_2O$ (3)

Three drops of triethanolamine were added to a solution of 0.027 g (0.10 mmol) $[Co(NH_3)_6]Cl_3$ and 0.045 g (0.20 mmol) sodium salt of 3-sulfobenzoic acid in H_2O (6 mL). The mixture was stirred for 5 min at room temperature, then placed in an ultrasonic bath and sonicated at 50 °C for 30 min. The resulting mixture was filtered and the mother liquor was allowed to evaporate slowly at room temperature in a sealed vial. Orange needle-like crystals **3** suitable for X-ray analysis were filtered after three months, washed with an ethanol/water (2 : 1) mixture and air-dried. Yield: 0.012 g (26% based on $[Co(NH_3)_6]Cl_3$). Elemental analysis calcd for **3**, $C_7H_{24}ClCoN_6O_9S$ (462.76 g mol^{-1}): C, 18.17; H, 5.23; N, 18.16%. Found. C, 17.87; H, 5.91; N, 18.00%. FT-IR (cm^{-1}): 3256 m, 3134 sh, 2952 sh, 2923 s, 2854 sh,1593 s, 1556 s, 1464 m, 1380 s, 1342 m, 1300 sh, 1174 vs, 1163 sh, 1102 s, 1078 sh, 1030 s, 997 m, 877 m, 761 m.

Synthesis of $[Co(NH_3)_6]_2(3\text{-sb})(SO_4)Cl_2{\cdot}7H_2O$ (4)

$[Co(NH_3)_6]Cl_3$ (0.027 g, 0.10 mmol) and the sodium salt of 3-sulfobenzoic acid (0.045 g, 0.20 mmol) were combined in a PTFE-lined reactor and dissolved in H_2O (6 mL) with three drops of triethanolamine by stirring the mixture for 10 min. Then the sample was secured in a steel autoclave and placed in a programmable oven for hydrothermolysis. The oven was heated up to 80 °C, the temperature was held for 6 h and then the oven was cooled to room temperature within 12 h. After opening the autoclave, the reaction mixture was filtered, and the mother liquor was allowed to evaporate slowly at room temperature in a sealed vial. Orange needle-like crystals **4** suitable for X-ray analysis were filtered after five months, washed with water and air-dried. Yield: 0.007 g (9% based on $[Co(NH_3)_6]Cl_3$). FT-IR (cm^{-1}): 3395 vs, 3158 vs, 2944 sh, 2901 h, 2841 sh, 1635 sh, 1592 m, 1545 m, 1488 m, 1460 m, 1401 sh, 1384 s, 1351 sh, 1326 s, 1304 sh, 1232 m, 1183 m, 1165 sh, 1095 s, 1080 m, 1066 sh, 1032 s, 1004 s, 916 m, 902 sh, 874 sh, 831 br.m, 769 m, 757 m, 683 sh, 666 m.

Synthesis of $\{[Co(NH_3)_6][Na(3\text{-sb})Cl_2]{\cdot}H_2O\}_n$ (5)

Three drops of 1,2-dimethyl imidazole were added to a solution of 0.027 g (0.10 mmol) $[Co(NH_3)_6]Cl_3$ and 0.020 g (0.09 mmol) sodium salt of 3-sulfobenzoic acid in an EtOH/H_2O (1 : 1) mixture (6 mL). The mixture was stirred for 5 min at room temperature, then placed in an ultrasonic bath and sonicated at 50 °C for 30 min. The resulting mixture was filtered and the mother liquor was allowed to evaporate slowly at room temperature in a sealed vial. Orange plate-like crystals **5** suitable for X-ray analysis were filtered after one month, washed with an ethanol/water solution (2 : 1) and air-dried. Yield: 0.013 g (31% based on the sodium salt of 3-sulfobenzoic acid). Elemental analysis calcd for **5**, $C_7H_{22}Cl_2CoN_6NaO_{5.69}S$ (466.18 g mol^{-1}): C, 18.01; H, 4.70; N, 18.01%. Found. C, 17.89; H, 4.32; N, 18.19%. FT-IR (cm^{-1}): 3477 sh, 3144 br.s, 2952 sh, 2923 s, 2854 sh, 1591 br.m, 1542 m, 1463 m, 1412sh, 1377 m, 1366 sh, 1354 m, 1324 vs, 1220 m, 1182 m, 1150 m, 1092 m, 1031 m, 998 w, 914 sh, 826 s, 755 m, 665 w.

Synthesis of $\{[Co(NH_3)_6][K_2(4\text{-sb})_2Cl]\}_n$ (6)

Three drops of triethanolamine were added to a solution of 0.027 g (0.10 mmol) $[Co(NH_3)_6]Cl_3$ and 0.048 g (0.2 mmol) potassium salt of 4-sulfobenzoic acid in an EtOH/H_2O (1 : 1) mixture (6 mL). The mixture was stirred for 5 min at room temperature, then placed in an ultrasonic bath and sonicated at 50 °C for 30 min. The resulting mixture was filtered and the mother liquor was allowed to evaporate slowly at room temperature in a sealed vial. Orange plate-like crystals **6** suitable for X-ray analysis were filtered after one month, washed with ethanol/water (2 : 1) and air-dried. Yield: 0.018 g (26% based on $[Co(NH_3)_6]Cl_3$). Elemental analysis calcd for **6**, $C_{14}H_{26}ClCoK_2N_6O_{10}S_2$ (675.11 g mol^{-1}): C, 24.88; H, 3.85; N, 12.44%. Found. C, 24.74; H, 3.84; N, 12.35%. FT-IR (cm^{-1}): 3507 sh, 3257 m, 3155 sh, 1631 sh, 1591 m, 1544 m, 1394 sh, 1377 m, 1351 m, 1331 sh, 1175 vs, 1144 sh, 1114 s, 1031 s, 1005 m, 864 m, 843 m, 774 w, 740 m, 693 w.

Synthesis of $[Co(NH_3)_6](Hssz)(ssz){\cdot}4H_2O$ (7)

Three drops of diethanolamine were added to a solution of 0.027 g (0.10 mmol) $[Co(NH_3)_6]Cl_3$ and 0.08 g (0.2 mmol) sulfasalazine in an EtOH/H_2O (1 : 1) mixture (6 mL). The mixture was stirred for 5 min at room temperature, then placed in an ultrasonic bath and sonicated at 50 °C for 30 min. The resulting mixture was filtered and the mother liquor was allowed to evaporate slowly at room temperature in a sealed vial. Orange block-like crystals 7 suitable for X-ray analysis were filtered after one week, washed with an ethanol/water solution (1 : 2) and air-dried. Yield: 0.068 g (66% based on $[Co(NH_3)_6]Cl_3$). Elemental analysis calcd for 7, $C_{36}H_{46}CoN_{14}O_{14}S_2$ (1021.92 g mol^{-1}): C, 42.31; H, 4.54; N, 19.19%. Found. C, 42.32; H, 4.74; N, 18.86%. FT-IR (cm^{-1}): 3286 br.w, 2967 m, 2928 sh, 2869 sh, 1599 vs, 1532 sh, 1471 s, 1424 vs, 1371 s, 1360 sh, 1286 m, 1241 m, 1162 m, 1133 m, 1120 sh, 1084 m, 1052 s, 1005 sh, 977 sh, 963 sh, 834 sh, 801 s, 775 sh.

X-ray crystallography

Single-crystal X-ray diffraction experiments for **1–7** were performed at 293 K on an Xcalibur E CCD diffractometer using graphite-monochromatized Mo Kα radiation. The position of most of the non-hydrogen atoms was located by direct methods. The remaining atoms were found in an alternating series of least-square cycles and difference Fourier maps. The positions of hydrogen atoms in the structures were located on difference Fourier maps or calculated geometrically and refined isotropically. The location of the NH_3 hydrogen atoms in **1–7** were optimized by means of a SHELXL "AFIX 137" card. All non-hydrogen atoms were refined in the full-matrix anisotropic approximation using the SHELX software package.[44] The crystal structure of compound **7** revealed the presence of one ordered water molecule per formula unit as well as a channel-like region with 13 highly disordered water solvent molecules with partial occupancy positions with SOF values from 0.5 to 0.113. These molecules have been refined in the isotropic model, resulting in a total number of disordered water molecules that is very close to 3 per formula unit. The disordered region was also verified by the PLATON SQUEEZE tool[45,46] and 107 electrons were found in a volume of 498 Å in 1 void per unit cell, corresponding to approximately 11 water molecules in the disordered region per unit cell or 5.5 per formula unit. The atomistic solvent disorder model was used to describe the structure, as it allows the H-bonds of the hexaamminecobalt(III) cation with the water molecules in the disordered region to be estimated. The crystallographic data and refinement details of **1–7** are given in Tables 1 and S2.† The selected bond distances are listed in Table S3† and the geometry of the hydrogen bonds is given in Table S4.† The figures were drawn using the CCDC Mercury 2024.1.0 program.[47]

Hirshfeld surface calculations

The intermolecular interactions in compounds **1–7** were analyzed using Hirshfeld surface analysis, as detailed in ref. 48 and 49, utilizing the CrystalExplorer program.[50] The methodology employed for the quantification and elucidation of intermolecular interactions within the crystal packing of these compounds included the application of the normalized contact distance d_{norm} (illustrated in Fig. S16–S18†) and two-dimensional (2D) fingerprint plots (depicted in Fig. S19†). The graphical plots were mapped with d_{norm} using a red–white–blue scheme. The intense red color indicates contacts that are shorter than the sum of van der Waals radii, while the white color highlights contacts that fall within the van

Table 1 Crystal data and details of structural determinations for **1–7**

	1	**2**	**3**	**4**
Formula	$C_{20}H_{35}CoN_{10}O_{12}S_4$	$C_{14}H_{32}ClCoN_{10}O_6S_2$	$C_7H_{24}ClCoN_6O_9S$	$C_7H_{53}Cl_2Co_2N_{12}O_{16}S_2$
M_r/g mol^{-1}	794.75	594.99	462.76	814.49
Cryst. system	Orthorhombic	Triclinic	Orthorhombic	Triclinic
Space group	*Fddd*	*P*$\bar{1}$	*Pnma*	*P*$\bar{1}$
a/Å	14.9159(12)	7.4363(6)	25.0699(10)	7.4383(5)
b/Å	18.4135(9)	8.2733(6)	7.2512(4)	12.0736(9)
c/Å	22.7514(13)	11.5486(14)	10.8265(6)	19.2979(12)
α/°	90	110.849(9)	90	100.100(6)
β/°	90	94.899(8)	90	98.038(6)
γ/°	90	90.864(6)	90	91.656(6)
V (Å^3)	6248.8(7)	660.76(11)	1968.12(17)	1686.9(2)
Z	8	1	4	2
Final R_1, wR_2	0.0442, 0.1212	0.0353, 0.0899	0.0485, 0.1471	0.0579, 0.1316
R indices R_1, wR_2 (all data)	0.0553, 0.1278	0.0453, 0.0977	0.0584, 0.1559	0.1017, 0.1601
CCDC	2415770	2415775	2415776	2415772
	5	**6**	**7**	
Formula	$C_7H_{22}Cl_2CoN_6NaO_{5.69}S$	$C_{14}H_{26}ClCoK_2N_6O_{10}S_2$	$C_{36}H_{46}CoN_{14}O_{14}S_2$	
M_r/g mol^{-1}	466.18	675.11	1021.92	
Cryst. system	Monoclinic	Tetragonal	Triclinic	
Space group	$P2_1/m$	*I*4/*m*	*P*$\bar{1}$	
a/Å	14.489(3)	14.3265(5)	12.9654(5)	
b/Å	6.8710(10)	14.3265(5)	13.1933(6)	
c/Å	17.692(3)	24.7933(16)	16.5514(9)	
α/°	90	90	83.432(4)	
β/°	97.903(17)	90	72.016(4)	
γ/°	90	90	68.761(4)	
V (Å^3)	1744.6(5)	5088.8(5)	2510.0(2)	
Z	4	8	2	
Final R_1, wR_2	0.0528, 0.0847	0.0435, 0.1095	0.0648, 0.1764	
R indices R_1, wR_2 (all data)	0.1081, 0.0902	0.0621, 0.1200	0.1000, 0.2021	
CCDC	2415773	2415771	2415774	

der Waals separation range. Longer contacts are represented by blue. The 2D fingerprint plots were presented in an expanded view of 0.6–2.8 Å, with the scales for the d_i (inside) and d_e (outside) distances indicated on the axes of the plot.

Computational details

Decomposition analysis of the intermolecular interaction energy (E_{int}) was carried out using the symmetry adapted perturbation theory (SAPT) method[51–54] to gain insight into the non-covalent bonding interactions between $[Co(NH_3)_6]^{3+}$ cations and various aromatic sulfonic acid derivatives in **1**–**7**. This method allows decomposition of the interaction energy into different terms, such as electrostatic, exchange, induction, and dispersion, and can be expressed within the framework of the SAPT method as $E_{int} = E_{elst} + E_{exch} + E_{ind} + E_{disp}$, where E_{elst} is the classical Coulomb interaction between fragments, with positive or negative values; E_{exch} is the short-range exchange repulsion between fragments, with positive values (*i.e.* unfavorable for binding); E_{ind} reflects the polarization and transfer of charges between fragments, with a negative value; E_{disp} has a negative value and acts as an attractive force. All SAPT calculations were done with the Psi4 software using density fitting at the sSAPT0/jun-cc-pVDZ level, and the aug-cc-pVDZ basis set was used for cobalt atoms.[51]

Results and discussion

Synthetic aspects and preliminary characterization

Our previous research[40] demonstrated that the reaction of $[Co(NH_3)_6]Cl_3$ with various organic N-, N,O-, and O-donor moieties occurs exclusively only in the presence of triethanolamine, sodium azide, or 1,3,5-triazine. The current series of compounds (**1**–**7**) was obtained through the crystallization of hexaamminecobalt(III) chloride with aromatic sulfonic acid derivatives such as 3-pyridinesulfonic acid, the sodium salt of 3-sulfobenzoic acid, the potassium salt of 4-sulfobenzoic acid, or sulfasalazine under different conditions, but in all cases with the addition of triethanolamine (**1**–**4** and **6**), 1,2-dimethylimidalzole (**5**), or diethanolamine (**7**). Stirring of the starting cobalt(III) components with 3-pyridinesulfonic acid in water at 50 °C for 30 min in the presence of triethanolamine results in the crystallization of **1** with a yield of 43%, and the same raw material in a methanol/acetonitrile mixture leads to the formation of compound **2** with a yield of 24%. Moreover, the application of ultrasonic irradiation to the starting components in ethanol/water solutions, or simply in water in the presence of triethanolamine (**3**, **6**), 1,2-dimethylimidazole (**5**), and diethanolamine (**7**) has also facilitated the formation of orange crystals with this cation, with yields ranging from 26% to 66%. The hydrothermal synthesis of the starting components in the presence of triethanolamine yielded crystals of **4**, with a yield of only 9%. Additionally, the reactions were conducted without triethanolamine, diethanolamine, and 1,2-dimethylimidazole, and it was observed that the synthesis of compounds without these components did not result in the formation of diffraction-quality crystals.

The IR spectra of compounds **1**–**7** (Fig. S2–S8†) reveal the presence of characteristic bands for the coordinated ammonia (NH_3) molecules of the $[Co(NH_3)_6]^{3+}$ complex cation, exhibiting absorption within the range of 3159–3135 cm^{-1} due to asymmetric and symmetric stretching vibrations (ν_{as+s}(N–H)). Furthermore, the spectra exhibit absorption within the ranges of 1593–1570 cm^{-1} and 1342–1326 cm^{-1}, which can be attributed to bending vibrations (δ_{as}(HNH) and δ_s(HNH), respectively). Finally, a pronounced band at 877–825 cm^{-1} is evident, which can be attributed to in-plane and out-of-plane rocking vibrations, $\rho_r(NH_3)$. These observations are consistent with those documented in the precursor $[Co(NH_3)_6]Cl_3$ (Fig. S1†), exhibiting slight displacements due to the formation of hydrogen bonds in the corresponding compounds as well as previously reported {$Co(NH_3)_6$]-based multi-component compounds.[40] This displacement may also contribute to the formation of supramolecular motifs. The asymmetric and symmetric C–H stretching vibrations from organic ligands were identified within the range of 2967–2841 cm^{-1}. In compounds **1** and **6**, these vibrations exhibited an overlap with strong vibrations of the amine groups from the complex cation $[Co(NH_3)_6]^{3+}$. In **1** and **2**, the ring stretching vibrations of the pys^- anion occur in the general region of 1623–1400 cm^{-1}.[55] These are superimposed with the deformation oscillations of the amine groups in this region. Asymmetric and symmetric stretching vibrations of the deprotonated carboxylic group of the sulfobenzoate ion in compounds **3**–**6** were observed in the region 1670–1542 cm^{-1} and 1488–1460 cm^{-1}, respectively, as weak and medium bands that overlap with the δ(HNH) vibration. In contrast, the asymmetric and symmetric stretching vibrations of the protonated and deprotonated carboxylic groups from sulfasalazine in **7** manifested as very strong bands at 1599 and 1424 cm^{-1}, respectively. The asymmetric and symmetric stretching vibrations of sulfonic groups are found in the region of 1395–1379 cm^{-1} and 1189–1004 cm^{-1}, respectively.[56]

Structural analysis

All the compounds **1**–**7** were characterized by the single crystal X-ray diffraction method. Compounds **1** and **3** crystallize in the orthorhombic space groups *Fddd* and *Pnma*, respectively, compound **5** in the monoclinic space group $P2_1/m$, compound **6** in the tetragonal space group $I4/m$, and the other compounds in the triclinic space group $P\bar{1}$ (Table 1). The compounds are ionic and multi-component, formed by hydrogen bonds between the complex cations, anions, and solvation molecules as well as by coordination bonds with alkali metals in compounds **5** and **6**. In all structures, the cobalt(III) cations are coordinated to six ammonia molecules at the vertices of an octahedron, with Co–N distances ranging from 1.944 to 1.984 Å. These distances are comparable with those observed in related compounds for the $[Co(NH_3)_6]^{3+}$

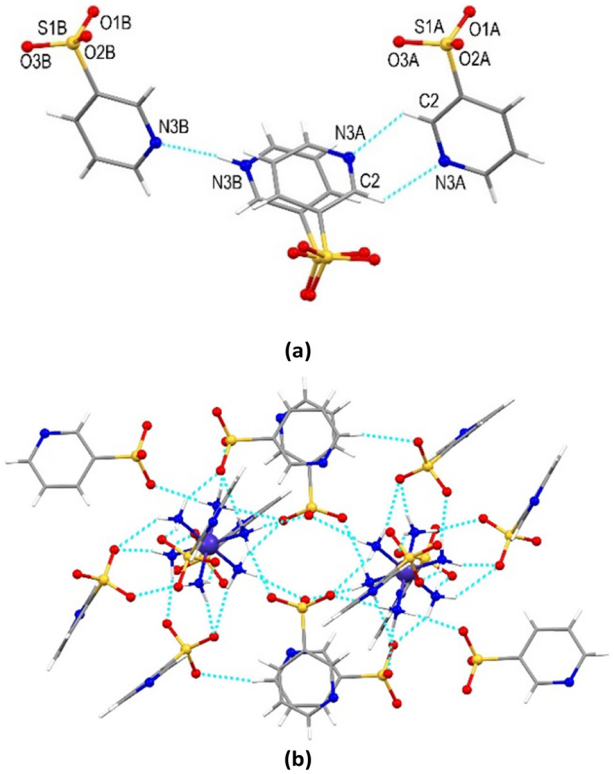

Fig. 1 (a) The H-bonds between the disordered pys^- anions and the neutral Hpys molecule in **1**. (b) H-bonding interactions around $[Co(NH_3)_6]^{3+}$ cations in the structure of **1**. Hydrogen bonds are shown as blue dashed lines.

complex cation.[19,31,39,40] It is noteworthy that in all cases, except **4**, the Co(III) complex cation provides all 18 hydrogen atoms for hydrogen bond formation. Furthermore, the presence of charge-assisted hydrogen bonds of N–H···O type between the amine ligands and the sulfonate groups in the structure is a common feature for all compounds **1–7**.

The compound $[Co(NH_3)_6](pys)_3{\cdot}Hpys$ (**1**) is composed of a $[Co(NH_3)_6]^{3+}$ cation, a pys^- anion, and a neutral Hpys molecule in zwitterion form with a 1:3:1 stoichiometry (Fig. 1a). The cation is located at the intersection of three twofold axes. The asymmetric part of the unit cell comprises one quarter of the cation, three quarters of the pys^- anion, and one quarter of the neutral Hpys molecule (Fig. S9a†). In the model of structure, the pys^- anion and the neutral Hpys molecules in the asymmetric part of the unit cell are located at approximately the same place, overlap almost completely, and differ mainly in the position of the nitrogen atom, N3A and N3B. In each of these two close positions A and B, the organic components have been refined with a site occupancy factor of 0.5. In position A (N3A), the neighboring twofold related pys^- anions are linked by a couple of C(2)–H···N(3A) bonds with a distance of 2.941(8) Å. In position B (N3B), the neighboring twofold related components form an N(3B)–H···N(3B) = 2.879(8) Å bond, as illustrated in Fig. 1a. Only one N3B in such a dimer is protonated. However, since these components are symmetry related and indistinguishable from a structural point of view, the H atom should be statistically distributed between these two equivalent nitrogen atoms, providing a charge balance in the structure because one of the components is charged and another one is neutral. The disordered model with 'half' H atoms has been used in refinement.

In the crystal structure, each $[Co(NH_3)_6]^{3+}$ cation is surrounded by and H-bonded with six pys^- anions and two Hpys zwitterions, and each pys^-/Hpys is hydrogen-bonded to two neighboring $[Co(NH_3)_6]^{3+}$ cations. All 18 hydrogen atoms of the hexaamminecobalt cation are involved in N–H···O hydrogen bonds with SO_3^- groups, forming a 3D hydrogen-bonded network in **1** (Table S4† and Fig. 1b and S9b†). The pys^- and Hpys components exhibit infinite π···π stacking interactions between their pyridine moieties along the [101] and [10–1] directions, with a centroid···centroid distance ranging from 3.225 to 4.044 Å (Fig. S9c†).

The crystals of compound **2**, $[Co(NH_3)_6](pys)_2Cl{\cdot}2MeCN$, are composed of a complex cation $[Co^{III}(NH_3)_6]^{3+}$, pys^- and Cl^- anions, and solvent MeCN molecules with a 1:2:1:2 stoichiometry, so unlike **1**, comprise two different anionic components (Fig. S10b†). The asymmetric part of the unit cell comprises half of the $[Co(NH_3)_6]^{3+}$ cation and half of the Cl^- anion, which reside on inversion centers, a pys^- anion, and a MeCN molecule (Fig. S10a†). The ionic components within the crystal are associated by charge-assisted extended N–H···O hydrogen bonds. All 18 hydrogen atoms of the $[Co(NH_3)_6]^{3+}$ cation are involved in the formation of these hydrogen bonds (Table S4†). Each cation is surrounded by four pys^- anions and each pys^- anion serves as a bridge between cations, forming an N–H···O hydrogen-bonded chain along the *a* axis (Fig. S10c and d†). Additionally, chloride anions bridge cations by N–H···Cl H-bonds along the *b* axis, facilitating the formation of a 2D hydrogen-bonded layer, as shown in Fig. 2a and S10e.† The hydrophilic H-bonded components reside inside the layer and the hydrophobic ones on its surfaces. In the crystal, the parallel layers are stacked along the *c* axis, creating infinite hourglass-shaped channels along the *b* axis. These channels are filled with acetonitrile solvent molecules (Fig. 2b).

The synthesis of compounds **3–6** with hexaamminecobalt(III) chloride has been achieved through the use of the sodium salt of 3-sulfobenzoic acid and the potassium salt of 4-sulfobenzoic acid. These organic anions possess an additional functional group, such as a carboxylate group, which, in combination with the sulfonate group, may serve as both mono- and dianion, thus allowing for the modulation of the functionality of the final materials with a wide range of structural motifs and properties.

The orthorhombic crystals (space group *Pnma*) of compound **3**, $[Co(NH_3)_6](3\text{-sb})Cl{\cdot}4H_2O$, comprise $[Co(NH_3)_6]^{3+}$ cations, 3-sb^{2-} dianions, Cl^- anions, and water molecules in a 1:1:1:4 stoichiometry (Fig. S11b†). The asymmetric unit of **3** consists of half of the $[Co(NH_3)_6]^{3+}$ cation, half of the organic dianion derived from deprotonated 3-sulfobenzoic acid, half of the Cl^- anion, and one solvate water molecule,

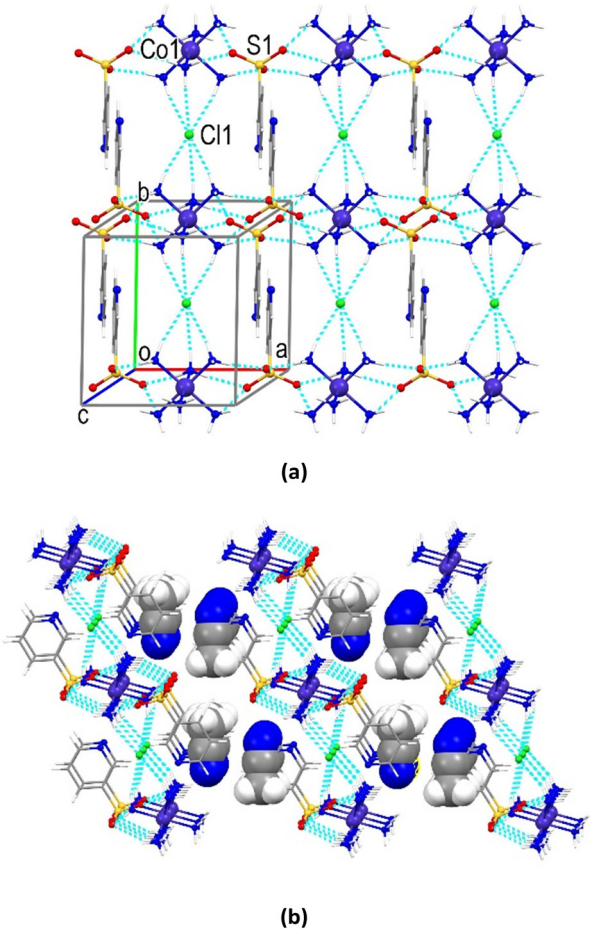

Fig. 2 (a) Formation of a supramolecular layer in the structure of **2**. (b) Stacking of layers along the *c* axis and formation of channels with solvent MeCN molecules. Hydrogen bonds are shown as blue dashed lines.

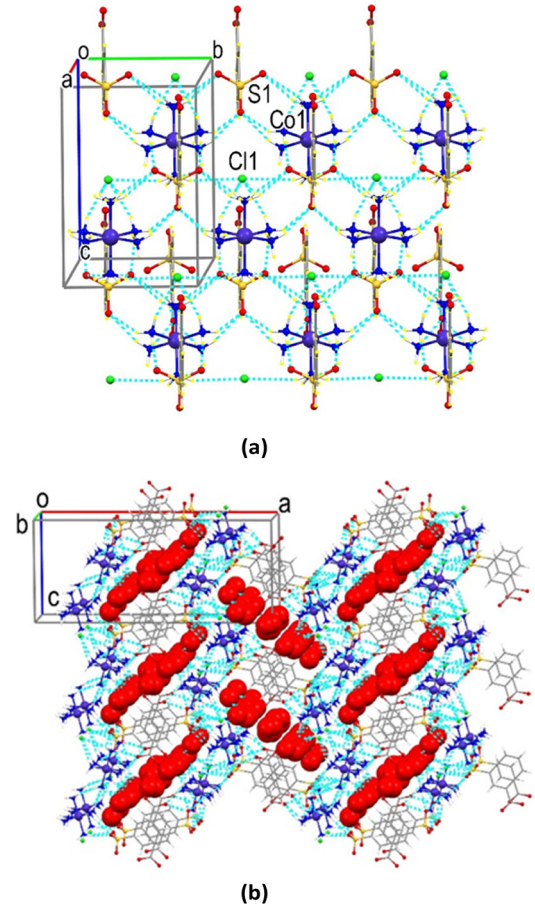

Fig. 3 (a) A fragment of the supramolecular layer in which the $[Co(NH_3)_6]^{3+}$ cations are linked by H-bonds with the Cl^- anions and oxygen atoms of the sulfonate groups in **3**. (b) Formation of channels in the crystal due to bridging of layers by N–H···O bonds of sulfonate and carboxylate groups of 3-sb. The solvent water molecules are shown in a space-filling mode, and hydrogen bonds are depicted as blue dashed lines.

all residing on the mirror plane (Fig. S11a†). The cation forms hydrogen N–H···O bonds with four 3-sb^{2-} anions, involving oxygen atoms from three sulfonate groups and one oxygen atom from the carboxylate group of the fourth 3-sb. Additionally, it forms three N–H···Cl bonds with chloride anions and three N–H···O bonds with disordered water molecules, saturating all 18 of its possible H-bonds (Fig. S11c and Table S4†). The 3-sb^{2-} dianion is connected to three $[Co(NH_3)_6]^{3+}$ cations by N–H···O bonds originating from the sulfonate group, and to one cation by an oxygen atom of the carboxylate group (Fig. S11d†). The chloride anion is connected by N–H···Cl bonds with three neighboring cations. The hydrogen bonds of the $[Co(NH_3)_6]^{3+}$ cations with the sulfonate groups and chloride anions result in the formation of a well-defined supramolecular layer parallel to the *bc* plane (Fig. 3a).

In the crystal, neighboring layers are linked by 3-sb^{2-} anions *via* H-bonds of sulfonate and carboxylate groups with cations, thus uniting the layers in a 3D supramolecular motif and forming the channels parallel to the *b* axis that are filled by both ordered and disordered water solvent molecules (Fig. 3b). The 3-sb^{2-} anions reside in parallel planes separated by 3.626 Å and show the formation of infinite π···π stacking of aromatic moieties with a centroid···centroid separation of 4.031 Å (Fig. S11e†).

Compound **4**, $[Co(NH_3)_6]_2(3\text{-sb})(SO_4)Cl_2{\cdot}7H_2O$, consists of $[Co(NH_3)_6]^{3+}$ cations, 3-sb^{2-} and SO_4^{2-} dianions, chloride anions, and water molecules with a 2:1:1:2:7 stoichiometry. In comparison to compound **3**, compound **4** differs by the presence of the sulfate anion, which forms under hydrothermal heating of the starting precursors, and inorganic components essentially predominate in the composition. The crystal structure of **4** reveals the existence of three crystallographically independent $[Co(NH_3)_6]^{3+}$ cations (Co2, Co1, and Co3): one in the general position and two in the special ones on the inversion centers (Fig. 4 and S12a†).

Similar to **3**, the cation in the general position (Co2) forms N–H···O hydrogen bonds with four 3-sb^{2-} anions, involving oxygen atoms from three different sulfonate groups and one oxygen atom from the carboxylate group. However, the further environment is different, exhibiting H-bonds with

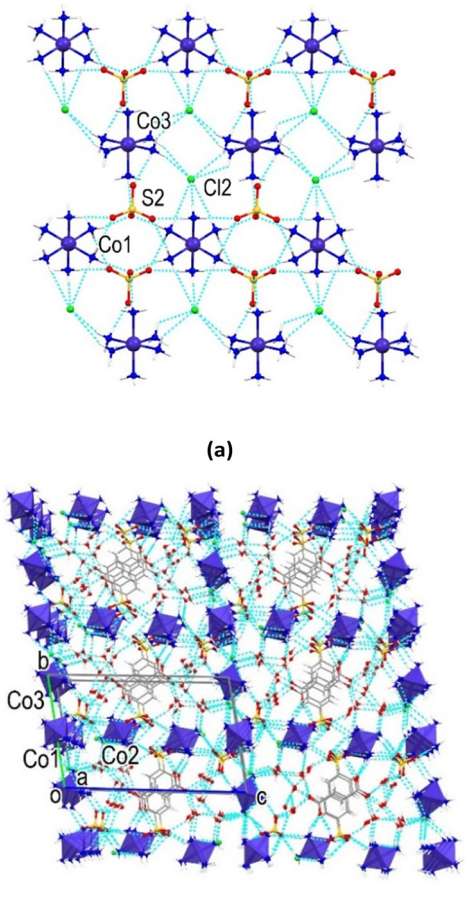

Fig. 4 (a) View of an inorganic layer formed between Co(III) hexaammine cations (Co1 and Co3) and SO_4^{2-} and Cl^- anions in **4**. (b) A 3D hydrogen-bonded network formed by charged and neutral components. Co atoms are shown in polyhedral presentation. Hydrogen bonds are shown as blue dashed lines.

two chloride anions, one sulfate anion, and two water molecules. Only 17 hydrogen atoms out of 18 possible participate in these H bonds (Table S4†). One of the cations, situated in a special position (Co1), is surrounded by and H-bonded with four sulfate dianions and two chloride anions, using all 18 hydrogen atoms of the cation. The second one in the special position (Co3) is surrounded by and H-bonded with two sulfate dianions, four chloride anions, and four water molecules, involving all H atoms of the cation (Fig. S12b and Table S4†). The inorganic component, comprising centrosymmetric hexaamminecobalt(III) cations (Co1 and Co3), sulfate and chloride anions linked by charge-assisted H-bonds, forms well-defined pure inorganic supramolecular layers oriented parallel to the *ab* plane (Fig. 4a). The structural role of the 3-sb^{2-} dianions is comparable to that observed in compound **3**. In **4**, the 3-sb^{2-} dianions are also linked to three $[Co(NH_3)_6]^{3+}$ cations by N–H···O bonds of the sulfonate group and to another cation by an oxygen atom of the carboxylate group (Fig. S12c†). Similar to **3**, the center symmetry-related 3-sb^{2-} dianions in **4** are situated in parallel planes, separated by 3.537 and 3.612 Å, and alternate in an antiparallel mode. They partially overlap and form infinite π···π stacking along the *a* axis with centroid···centroid separations of their aromatic moieties of 4.526 and 3.982 Å (Fig. S12c†).[57] The H-bonded charged components in **4** form infinite channels along the *a* axis, which are filled by water solvent molecules (Fig. S12d†).

Compounds **5**, $\{[Co(NH_3)_6][Na(3\text{-sb})Cl_2]\cdot H_2O\}_n$, and **6**, $\{[Co(NH_3)_6][K_2(4\text{-sb})_2Cl]\}_n$, were obtained by crystallization from a solution of the corresponding starting precursors in EtOH/H_2O and subjected to sonication. Their structure revealed the formation of alkali metals containing coordination polymers (Fig. 5 and 6). In the case of the monoclinic crystals of compound **5**, all ionic components in the structure reside in special positions on mirror planes of the space group $P2_1/m$ and the asymmetric part of the unit cell contains two halves of $[Co(NH_3)_6]^{3+}$ and Na^+ cations, two halves of 3-sb^{2-} dianions, four halves of Cl^-, and disordered water solvent molecules (Fig. S13a†). The crystal structure reveals two types of similar but symmetry-independent negatively charged $[Na(3\text{-sb})Cl_2]^{3-}$ double-stranded polymeric chains, all running along the *b* axis and each involving only symmetry-related sodium atoms, Na1 or Na2 (Fig. 5a and

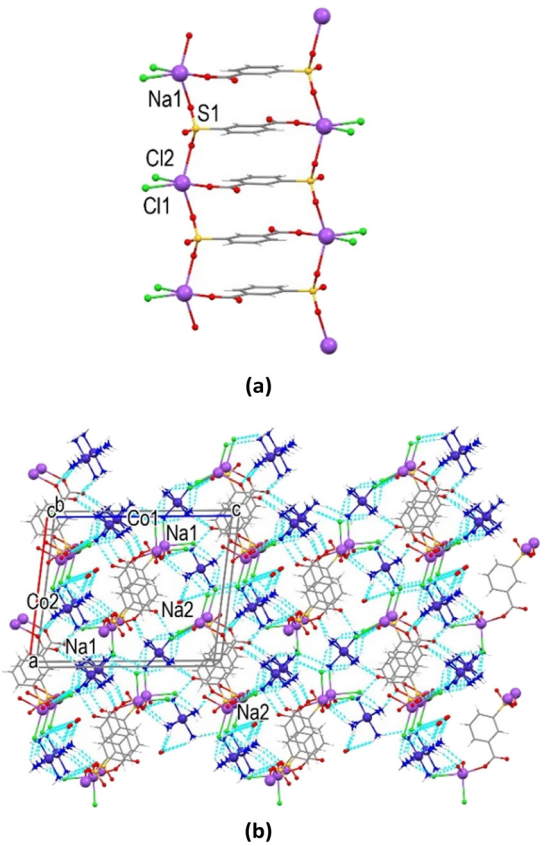

Fig. 5 (a) View of a double-stranded polymeric chain (Na1) in **5**. (b) Crystal packing illustrates the formation of a 3D supramolecular network from polymeric chains. Hydrogen bonds are shown as blue dashed lines.

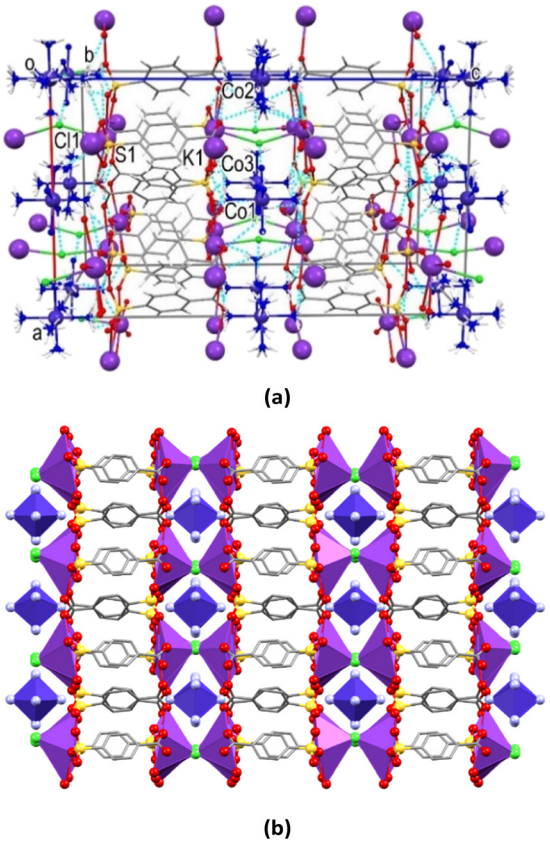

Fig. 6 (a) The crystal packing illustrates the formation of a 3D coordination polymer network in **6**. Hydrogen bonds are shown as blue dashed lines. (b) View of 3D coordination network along the *b* axis. Metal atoms are shown in polyhedral presentation. Hydrogen atoms are omitted for clarity.

S13b†). The chains are formed by the coordination of the 3-sb^{2-} anion to three sodium cations through sulfonate and carboxylate groups. The sodium atoms have Cl_2O_3 surrounding due to coordination three 3-sb^{2-} anions *via* oxygen atoms of two sulfonate groups and one carboxylate group, and two Cl^- anions. The coordination Na1 is intermediate between square planar and trigonal pyramidal, with a distortion parameter of τ = 0.489, and is more closely related to square planar for Na2, τ = 0.358 (τ = 1 for a trigonal pyramidal and τ = 0 for a square planar geometry). The 3-sb^{2-} anions inside the chains show infinite π···π stacking interactions with interplanar separation of their mean planes of 3.436 Å and centroid···centroid distances in the range of 3.722–3.757 Å (Fig. S13b†). The double-stranded chains interconnected by charge-assisted H-bonds with $[Co(NH_3)_6]^{3+}$ cations, resulting in the formation of a 3D hydrogen-bonded network (Fig. 5b and S13c†). Each of the two symmetry-independent hexaamminecobalt(III) cations is H-bonded to five chloride anions and two 3-sb^{2-} dianions, and the cations associated with Co2 show additional hydrogen bonding with partial occupancy disordered water solvent molecules. All 18 hydrogen atoms of $[Co(NH_3)_6]^{3+}$ cations participate in H-bonds (Table S4†).

Tetragonal crystals of compound **6** contain larger in size potassium alkali cations and 4-sb^{2-} organic dianions instead of 3-sb^{2-} ones compared to those observed in **5**. In the crystal, cobalt atoms (Co1, Co2, and Co3) of hexaamminecobalt(III) cations reside on the intersection of the fourfold axes and mirror planes, and chloride anions reside on the mirror plane of symmetry of the space group *I*4/*m* (Fig. S14a†). The 4-sb^{2-} dianions and potassium cation are located in general positions. The potassium atom coordinates four 4-sb^{2-} anions, two of which are bound by the oxygen atom of the sulfonate group in monodentate and chelate modes, while the remaining two are attached *via* the carboxylate groups in a monodentate mode. All five oxygen atoms are close to common mean plane, and the maximal deviation is 0.132 Å. The potassium atom is displaced from this plane by a distance of only 0.096 Å toward the chloride anion at the apical position. The coordination polyhedron of the potassium atom exhibits the rare pentagonal pyramid configuration observed for this atom (Fig. S14b†).

The 4-sb^{2-} dianions coordinate to the potassium cations through their sulfonate and carboxylate groups, linking them in layers parallel to the *ab* plane and also bridging two neighboring layers in the walls with hydrophilic components on their surfaces and hydrophobic ones inside. The parallel walls are perpendicular to the *c* axis. The chloride anions bridge such walls along the *c* axis, resulting in a 3D anionic network with α-polonium-like topology (Fig. S14c and d†). The hexaamminecobalt(III) cations are located inside this network and interact by charge-assisted N–H···O and N–H···Cl bonds. All 18 hydrogen atoms of each $[Co(NH_3)_6]^{3+}$ cation participate in these H-bonds (Fig. 6 and Table S4†).

The triclinic crystals of compound **7** consist of $[Co(NH_3)_6]^{3+}$ cations, monodeprotonated ($Hssz^-$) in the imide form and bideprotonated (ssz^{2-}) sulfasalazine anions, and water solvate molecules in a 1:2:4 stoichiometry (Fig. S15a†). The organic anions in this compound are the bulkiest of the organic anions reported here, and both mono- and dianions have similar angular conformation. The cation $[Co(NH_3)_6]^{3+}$ is N–H···O and N–H···N bonded with six anions: four ssz^{2-} and two $Hssz^-$. One of the four ssz^{2-} dianions is linked to the cation *via* two oxygen atoms of the carboxylic group and an oxygen atom of its hydroxylic group, two of the dianions *via* an oxygen atom of the sulfonamide group, and in addition, one of them *via* its nitrogen imide atom, and the remaining one *via* an oxygen atom of the hydroxylic group (Fig. S15b†). One of the $Hssz^-$ monoanions forms H-bonds with the cation *via* the oxygen atoms of the sulfonamide group, while another one *via* the oxygen atoms of the carboxylic group. The cationic environment is completed by a well-defined H-bond with the water molecule and also by three H-bonds with highly disordered water molecules, thus involving all 18 hydrogen atoms of the cation in H-bonding. In the crystal, two center symmetry-related $Hssz^-$ monoanions are linked by two N–H···N bonds, with the participation of the pyridine and sulfonamide groups, to form a supramolecular synthon $R_2^2(8)$[41,58] (Fig. S15c†).

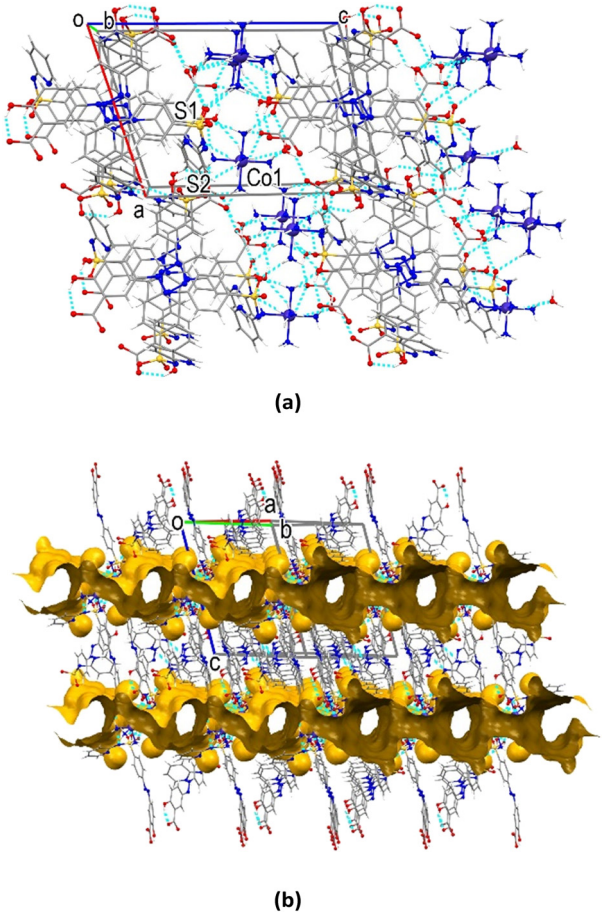

Fig. 7 (a) The crystal packing illustrates the formation of a 3D supramolecular network in **7**. (b) Channels in the crystal structure of **7**. Hydrogen bonds are shown as blue dashed lines.

The hydrogen-bonded ionic components form a supramolecular 3D structure with infinite channels running along the [−110] directions, which are filled with disordered water solvent molecules (Fig. 7). The formation of additional π···π interactions between the phenyl rings of neighboring $Hssz^-$ monoanions (centroid···centroid distance of 3.868 Å) as well as between neighboring ssz^{2-} dianions (centroid···centroid distance of 4.099 Å) contributes to the extended crystal packing in **7** (Fig. S15d†).

Hirshfeld surface analysis

The crystal packing of **1**–**7** is predominantly influenced by intermolecular hydrogen bonding interactions between the $\{Co(NH_3)_6]^{3+}$ cations and the corresponding organic moieties, anions, and solvate molecules. Nevertheless, the formation of the crystal structure depends on the interplay of diverse forces, which requires a comprehensive understanding of all intermolecular interactions within a given structure. A detailed examination of intermolecular close contacts in the structures of multi-component supramolecular compounds **1**–**7** was conducted using the highly effective Hirshfeld surfaces and 2D fingerprint plots, which provide valuable additional insight into the crystal structure. The organic components in the structure of the obtained compounds crystallized with protonated amine groups and deprotonated sulfonate groups (SO_3^-) for **1**, deprotonated sulfonate groups for **2**, both deprotonated sulfonate and carboxylate groups (SO_3^- and COO^-) for **3**–**6**, and both protonated amine groups and deprotonated carboxylate groups for **7**. Fig. S16–S18† illustrate the Hirshfeld surfaces around organic moieties mapped over d_{norm} and other properties, including shape index, curvedness, and fragment patch, for compounds **1**–**7**. The 2D fingerprint plots, which provide a quantitative summary of the nature and type of intermolecular contacts in **1**–**7**, are shown in Fig. 8 and S19.† In the crystal packing of compounds **1**–**6**, the O···H/H···O intermolecular interactions are the most predominant, accounting for 46.8% (**1**), 43.5% (**2**), 51.3% (**3**), 54.1% (**4**), 29.1% (**5**), and 28.9% (**6**) of the total

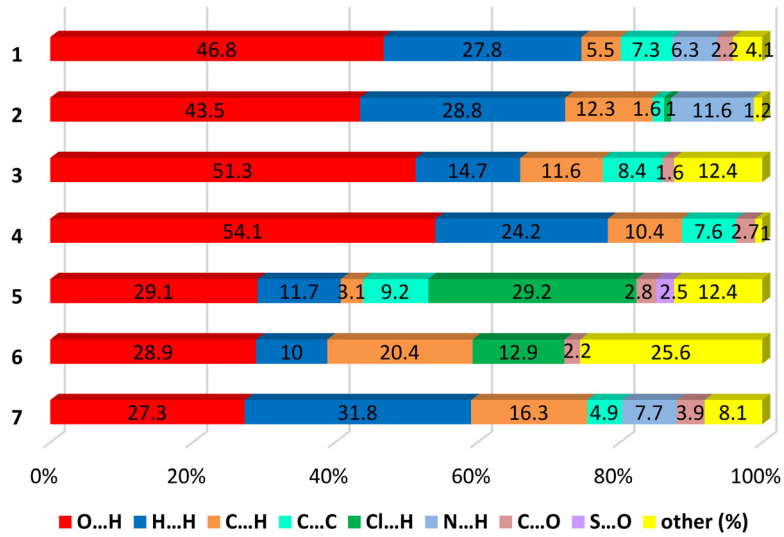

Fig. 8 Relative contributions to the Hirshfeld surface for the major intermolecular contacts in **1**–**7** around organic moieties.

interactions. In contrast, for compound **7**, where the bulkiest and the more hydrophobic organic $Hssz^-$ and ssz^{2-} moieties are present, the most prevalent contributions of 31.8% refer to H···H contacts. The second category of interactions comprises H···H contacts, which account for 27.8%, 28.8%, 14.7%, and 24.2% of the total interactions for compounds **1–4**, respectively. In the case of compound **5**, the most frequent interactions with a percentage of 29.2%, correspond to H···Cl/Cl···H contacts. hese H···Cl/Cl···H interactions are also present in other chlor-containing multi-component compounds **2**, **3**, and **6** (Fig. 8 and S19†). In **7**, the second category of interactions comprises O···H/H···O contacts (27.3%). Additionally, π···π (C···C) interactions contribute significantly to the total Hirshfeld surfaces of **1** (7.3%), **3** (8.4%), **4** (7.6%), **5** (9.2%), and **7** (4.9%). Furthermore, the presence of C–H···π interactions, as reflected in the contributions of the C···H/H···C contacts, was observed in all compounds (Fig. 8).

Calculation of interaction energy

In all studied compounds as well as in ref. 40, the bulky $[Co(NH_3)_6]^{3+}$ cations play a main role in the self-organization of multi-component supramolecular systems owing to the formation of hydrogen bonds with anions and solvation molecules. It was found in ref. 40 that the calculated binding energy in two-component systems in which hexaamminecobalt(III) is hydrogen-bonded with mono- and dianions as well as neutral molecules correlates with the biological activity of the given compounds. In the crystals, the cations are surrounded by anions, forming N–H···O hydrogen bonds, therefore the calculation of E_{int} has been performed for all observed cation–anion pairs (Table S5† and Fig. 9 and S20†).

It was shown that the cocrystals of the compound $[Co(NH_3)_6]Cl_3{\cdot}2(phen){\cdot}3H_2O$ (where phen is neutral 1,10-phenanthroline) possess biological activity against bacterial cancer in plants and the calculated absolute value of binding energy between the cation and the neutral ligand, linked by hydrogen bonds, is minimal among the studied compounds.[40] Therefore, Table 2 represents the interaction energy between those $[Co(NH_3)_6]^{3+}$ and anions, whose absolute values of E_{int} are minimal for each compound **1–7**. The absolute values of the calculated interaction energies decrease in the following order, $E_3 > E_4 > E_7 > E_6 > E_5 > E_2 > E_1$, and the found minimal energy E_1 (239.433 kcal mol^{-1}) is significantly greater than that in the published compound $[Co(NH_3)_6]Cl_3{\cdot}2(phen){\cdot}3H_2O$ (73.915 kcal mol^{-1} (ref. 40). The mean values of hydrogen bonds in Table 2 are not correlated with absolute values of E_{int} because of the following order of d values: $d_6 > d_2 > d_1 > d_7 > d_4 > d_5 > d_3$. In all selected pairs, the electrostatic term dominates in the calculated binding energies, followed by induction interaction. The interaction energies of two-component systems in **1–7** and of the inactive compounds in ref. 40, with the exception of $[Co(NH_3)_6]Cl_3{\cdot}2(phen){\cdot}3H_2O$, are in the same order of magnitude because they are in ranges of −239.433–−354.788 kcal mol^{-1} and −212.313–−448.3 kcal mol^{-1}, respectively. Thus, it can be assumed that compounds **1–7** will demonstrate reduced sensitivity to the oncogenic bacterium *Rhizobium* (*Agrobacterium*) *vitis* in comparison to $[Co(NH_3)_6]Cl_3{\cdot}2(phen){\cdot}3H_2O$.

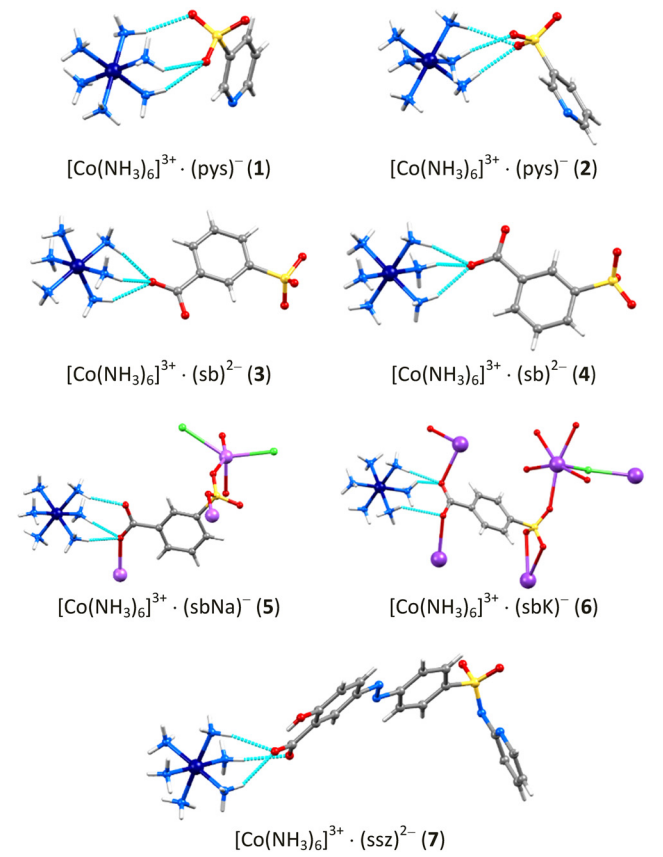

Fig. 9 View of the selected pairs for the estimation of their interaction energies.

Conclusions

The reaction of $[Co(NH_3)_6]Cl_3$ with organic ligands that contain sulfonic groups was investigated under a variety of synthetic conditions, including hydrothermal heating and ultrasonic treatment. The findings revealed that the formation of crystals of multi-component supramolecular compounds **1–7** can be facilitated by the inclusion of alcohol amines in the reaction mixture. Furthermore, the use of ultrasound during the synthesis with identical starting reagents, such as hexaamminecobalt(III) chloride and the sodium salt of 3-sulfobenzoic acid or the potassium salt of 4-sulfobenzoic acid, has been observed to promote the formation of alkaline-containing anionic coordination polymers in the case of compounds **5** and **6**. Compounds **1–4** and **7** exhibit a comparable crystal structure, wherein the $[Co(NH_3)_6]^{3+}$ cations serve as the fundamental building block for incorporating sulfonic derivatives, thereby facilitating the

Table 2 SAPT decomposition of the interaction energies (kcal mol^{-1}) for selected pairs in **1–7**

Selected pairs	O···H, Å	E_{elst}	E_{exch}	E_{ind}	E_{disp}	E_{int}	d^a (Å)
$[Co(NH_3)_6]^{3+}\cdot(pys)^-$ (**1**)	2.26	−219.496	11.409	−26.524	−4.821	−239.433	2.19
	2.18						
	2.14						
$[Co(NH_3)_6]^{3+}\cdot(pys)^-$ (**2**)	2.41	−221.058	11.760	−26.877	−4.879	−241.054	2.23
	2.15						
	2.13						
$[Co(NH_3)_6]^{3+}\cdot(sb)^{2-}$ (**3**)	2.10	−330.671	17.774	−36.515	−5.375	−354.788	2.09
	2.10						
	2.09						
$[Co(NH_3)_6]^{3+}\cdot(sb)^{2-}$ (**4**)	2.20	−326.317	15.753	−34.921	−4.952	−350.437	2.11
	2.10						
	2.04						
$[Co(NH_3)_6]^{3+}\cdot(sbNa)^-$ (**5**)	2.14	−231.629	12.898	−33.541	−4.933	−257.205	2.10
	2.08						
	2.08						
$[Co(NH_3)_6]^{3+}\cdot(sbK)^-$ (**6**)	2.64	−162.161	22.260	−154.438	−9.470	−303.809	2.37
	2.30						
	2.16						
$[Co(NH_3)_6]^{3+}\cdot(ssz)^{2-}$ (**7**)	2.18	−302.701	16.565	−35.018	−5.215	−326.368	2.15
	2.16						
	2.13						

[a] *d* – mean values of O···H hydrogen bonds.

formation of 1D, 2D, and 3D networks through the formation of extended charge-supported N–H···O bonds between amine ligands and sulfonate groups. The structure of compound **5** is composed of negatively charged $\{[Na(3\text{-sb})Cl_2]^{3-}\}_n$ double-stranded polymer chains linked by hydrogen bonds with $[Co(NH_3)_6]^{3+}$ cations, resulting in the formation of a 3D network *via* the combination of coordination and hydrogen bonds. The structure of compound **6** comprises a negatively charged $\{[K_2(4\text{-sb})_2Cl]^{3-}\}_n$ open coordination polymer 3D network incorporating the $[Co(NH_3)_6]^{3+}$ complex cations *via* H-bonds. Our studies show that the presence of alkali metal cations leads to the formation of anionic coordination polymers in the structure, ensuring at the same time that the $[Co(NH_3)_6]^{3+}$ cation saturates all its possible hydrogen bonds. Furthermore, the employment of the $[Co(NH_3)_6]^{3+}$ complex cations suggests the possibility of an effective synthetic strategy for the fabrication of metal–organic frameworks (MOFs) with precisely defined pores by the control of template sizes, such as that of the bulky hexaamminecobalt(III) cation. In the crystals of all compounds, in addition to extensive networks of hydrogen bond interactions of N–H···O(sulfonate) type, π···π stacking and C–H···π interactions also serve to stabilize the crystal packing. For the studied compounds, energy decomposition analysis of the intermolecular interaction energy for cation–anion pairs joined by hydrogen bonds was performed using the SAPT method and it was revealed that in all selected pairs, the electrostatic term dominates in the calculated binding energies, followed by induction interaction. The findings of the analysis indicated that compounds **1–7** exhibited a reduced level of inhibitory activity in comparison to the previously published compound of hexaamminecobalt(III) with 1,10-phenanthroline.[40] Consequently, these compounds will be less suitable for utilization against the oncogenic bacterium *Rhizobium* (*Agrobacterium*) *vitis*.

Data availability

The data supporting this article have been included as part of the ESI.† Crystallographic data for **1–7** have been deposited at the CCDC under 2415770 (**1**), 2415775 (**2**), 2415776 (**3**), 2415772 (**4**), 2415773 (**5**), 2415771 (**6**), and 2415774 (**7**) accession numbers.

Author contributions

ESB: chemical synthesis and growth of crystals, writing of the paper, analysis of the data. VChK: data collection and refinement, analysis of the data, generation of images, writing of the paper. YCh: formal analysis of the data. SGB: conceptualization, analysis of the data, generation of images, writing of the paper.

Conflicts of interest

There are no conflicts to declare.

Acknowledgements

The authors acknowledge the financial support from the Ministry of Education and Research of the Republic of Moldova (subprogram 011202).

Notes and references

1 A. K. Renfrew, E. S. O'Neill, T. W. Hambley and E. J. New, *Coord. Chem. Rev.*, 2018, **375**, 221.

2 T. Spataru and F. Fernandez, *Chem. J. Mold.*, 2016, **11**(1), 10.
3 K. Kar, D. Ghosh, B. Kabi and A. Chandra, *Polyhedron*, 2022, **222**, 115890.
4 P. A. Asbell, S. P. Epstein, J. A. Wallace, D. Epstein, C. C. Stewart and R. M. Burger, *Cornea*, 1998, **17**, 550.
5 T. Takeuchi, A. Böttcher, C. M. Quezada, T. J. Meade and H. B. Gray, *Bioorg. Med. Chem.*, 1999, **7**, 815.
6 J. A. Schwartz, E. K. Lium and S. J. Silverstein, *J. Virol.*, 2001, **75**, 4117.
7 S. P. Epstein, Y. Y. Pashinsky, D. Gershon, I. Winicov, C. Srivilasa, K. J. Kristic and P. A. Asbell, *BMC Opthalmol.*, 2006, **6**, 1.
8 E. L. Chang, C. Simmers and D. A. Knight, *Pharmaceuticals*, 2010, **3**, 1711.
9 A. P. King, H. A. Gellineau, S. N. MacMillana and J. J. Wilson, *Dalton Trans.*, 2019, **48**, 5987.
10 U. El-Ayaan and A. A. M. Abdel-Aziz, *Eur. J. Med. Chem.*, 2005, **40**, 1214.
11 P. Nagababu, J. N. L. Latha, P. Pallavi, S. Harish and S. Satyanarayana, *Can. J. Microbiol.*, 2006, **52**, 1247.
12 R. S. Kumar and S. Arunachalam, *Biophys. Chem.*, 2008, **136**, 136.
13 A. Mishra, N. K. Kaushik, A. K. Verma and R. Gupta, *Eur. J. Med. Chem.*, 2008, **43**(10), 2189.
14 E. D. Glowacki, M. Irimia-Vladu, S. Bauer and N. S. Sariciftci, *J. Mater. Chem. B*, 2013, **1**, 3742.
15 E. O. Schlemper, *J. Cryst. Mol. Struct.*, 1977, **7**, 81.
16 H. Brumm and M. Jansen, *Z. Anorg. Allg. Chem.*, 2001, **627**, 1433.
17 M. Gorol, N. C. Mosch-Zanetti, M. Noltemeyer and H. W. Roesky, *Z. Anorg. Allg. Chem.*, 2000, **626**, 2318.
18 S. A. Dalrymple, M. Parvez and G. K. H. Shimizu, *Inorg. Chem.*, 2002, **41**, 6986.
19 D. S. Reddy, S. Duncan and G. K. H. Shimizu, *Angew. Chem., Int. Ed.*, 2003, **42**, 1360.
20 R. P. Sharma, R. Bala, R. Sharma and P. Venugopalan, *J. Mol. Struct.*, 2004, **694**, 229.
21 R. P. Sharma, R. Bala, R. Sharma, B. M. Kariuki, U. Rychlewska and B. Warzajtis, *J. Mol. Struct.*, 2005, **748**, 143.
22 P. A. Brayshaw, A. K. Hall, W. T. A. Harrison, J. M. Harrowfield, D. Pearce, T. M. Shand, B. W. Skelton, C. R. Whitaker and A. H. White, *Eur. J. Inorg. Chem.*, 2005, 1127.
23 R. P. Sharma, R. Bala, R. Sharma and A. D. Bond, *Acta Crystallogr., Sect. C:Cryst. Struct. Commun.*, 2005, **61**, m356.
24 R. P. Sharma, R. Bala, R. Sharma and P. Venugopalan, *J. Mol. Struct.*, 2005, **752**, 170.
25 R. P. Sharma, R. Bala, R. Sharma and A. D. Bond, *Acta Crystallogr., Sect. E:Struct. Rep. Online*, 2006, **62**, m2113.
26 R. P. Sharma, R. Bala, R. Sharma, K. N. Singh and V. Ferretti, *J. Mol. Struct.*, 2006, **784**, 117.
27 S. A. Dalrymple and G. K. H. Shimizu, *Chem. Commun.*, 2006, 956.
28 E. Bernhardt, D. J. Brauer, M. Finze and H. Willner, *Angew. Chem., Int. Ed.*, 2006, **45**, 6383.
29 R. P. Sharma, R. Bala, R. Sharma, J. Perez and D. Miguel, *J. Mol. Struct.*, 2006, **797**, 49.
30 R. Bala, R. P. Sharma and A. D. Bond, *J. Mol. Struct.*, 2007, **830**, 198.
31 X.-Y. Wang, R. Justice and S. C. Sevov, *Inorg. Chem.*, 2007, **46**, 4626.
32 R. Bala, R. P. Sharma, P. Venugopalan and W. T. A. Harrison, *J. Mol. Struct.*, 2007, **830**, 8.
33 R. Bala, R. P. Sharma, U. Sharma, A. D. Burrows and K. Cassar, *J. Mol. Struct.*, 2007, **832**, 156–163.
34 I. Stein and U. Ruschewitz, *Z. Naturforsch., B:J. Chem. Sci.*, 2011, **66**, 471.
35 N. Gorska, A. Inaba, Y. Hirao, E. Mikul and K. Holderna-Natkaniec, *RSC Adv.*, 2012, **2**, 4283.
36 N. Gorska, A. Inaba, Y. Hirao and E. Mikuli, *J. Coord. Chem.*, 2013, **66**, 1238.
37 R. W. Seidel, R. Goddard, V. Gramm and U. Ruschewitz, *Z. Naturforsch., B:J. Chem. Sci.*, 2014, **69**, 277.
38 E. Roedern and T. R. Jensen, *Inorg. Chem.*, 2015, **54**, 10477.
39 Ch. Heering, B. Nateghi and C. Janiak, *Crystals*, 2016, **6**, 22.
40 M. Darii, E. S. Beleaev, V. Ch. Kravtsov, P. Bourosh, Y. Chumakov, J. Hauser, S. Decurtins, Sh.-X. Liu, O. Sultanova and S. G. Baca, *New J. Chem.*, 2022, **46**(23), 11404.
41 D. A. Haynes, J. A. Chisholm, W. Jones and W. D. S. Motherwell, *CrystEngComm*, 2004, **6**(95), 584.
42 A. A. Ganie, P. Vishnoi and A. A. Dar, *Cryst. Growth Des.*, 2019, **19**, 2289.
43 A. A. Ganie, A. A. Ahangar and A. A. Dar, *Cryst. Growth Des.*, 2019, **19**, 4650.
44 G. M. Sheldrick, *Acta Crystallogr., Sect. C:Struct. Chem.*, 2015, **71**, 3.
45 A. L. Spek, *Acta Crystallogr., Sect. D:Biol. Crystallogr.*, 2009, **65**, 148.
46 A. L. Spek, *Acta Crystallogr., Sect. C:Struct. Chem.*, 2015, **71**, 9.
47 C. F. Macrae, I. J. Bruno, J. A. Chisholm, P. R. Edgington, P. McCabe, E. Pidcock, L. Rodriguez-Monge, R. Taylor, J. van de Streek and P. A. Wood, *J. Appl. Crystallogr.*, 2008, **41**, 466.
48 F. L. Hirshfeld, *Theor. Chem. Acc.*, 1977, **44**, 129.
49 M. A. Spackman and D. Jayatilaka, *CrystEngComm*, 2009, **11**, 19.
50 P. R. Spackman, M. J. Turner, J. J. McKinnon, S. K. Wolff, D. J. Grimwood, D. Jayatilaka and M. A. Spackman, *J. Appl. Crystallogr.*, 2021, **54**, 1006.
51 J. M. Turney, A. C. Simmonett, R. M. Parrish, E. G. Hohenstein, F. A. Evangelista, J. T. Fermann, B. J. Mintz, L. A. Burns, J. J. Wilke, M. L. Abrams, N. J. Russ, M. L. Leininger, C. L. Janssen, E. T. Seidl, W. D. Allen, H. F. Schaefer, R. A. King, E. F. Valeev, C. D. Sherrill and T. D. Crawford, *Wiley Interdiscip. Rev.: Comput. Mol. Sci.*, 2012, **2**, 556.
52 B. Jeziorski, R. Moszynski and K. Szalewicz, *Chem. Rev.*, 1994, **94**, 1887.
53 T. Korona, R. Moszynski and B. Jeziorski, *J. Chem. Phys.*, 1996, **105**, 8178.
54 K. Szalewicz, *Wiley Interdiscip. Rev.: Comput. Mol. Sci.*, 2012, **2**, 254.

55 C. Y. Panicker, H. T. Varghese, D. Philip and H. I. S. Nogueira, *Spectrochim. Acta, Part A*, 2006, **64**, 744.
56 H. C. Garcia, R. Diniz and L. F. C. de Oliveira, *Polyhedron*, 2013, **53**, 40.
57 D. B. Ninković, G. V. Janjić, D. Veljković, D. N. Sredojević and S. D. Zarić, *ChemPhysChem*, 2011, **12**, 3511.
58 Sh. Huang, V. K. R. Cheemarla, D. Tiana and S. E. Lawrence, *Cryst. Growth Des.*, 2023, **23**, 5446.